ACS SENSORS

pubs.acs.org/acssensors

Article

PCR-Free Methodology for Detection of Single-Nucleotide Polymorphism with a Cationic Polythiophene Reporter

Muge Yucel, Altug Koc,* Ayfer Ulgenalp, Gun Deniz Akkoc, Metin Ceyhan, and Umit Hakan Yildiz*

Cite This: *ACS Sens.* 2021, 6, 950–957

Read Online

ACCESS | Metrics & More | Article Recommendations | Supporting Information

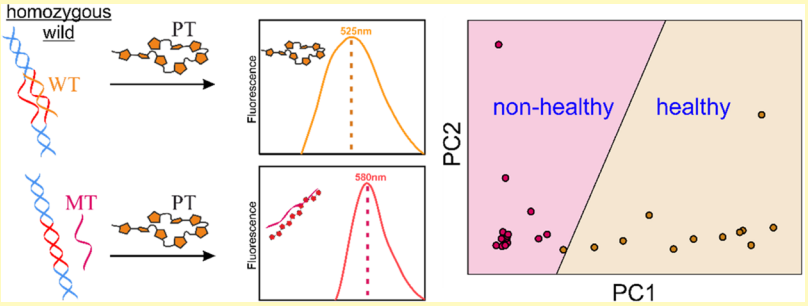

ABSTRACT: This study presents a nonamplification-based nucleic acid assay for the detection of single-nucleotide polymorphism (SNP) associated with familial Mediterranean fever (FMF) besides polymerase chain reaction (PCR)-based methodologies. The major objective is to show the potential of the proposed assay for rapid screening of FMF in a Mediterranean region of 400 million population. The assay relies on binding difference of specially designed wild and mutant primers to the target genomic DNA, followed by determination of unbound primers by quick titration of a cationic polythiophene reporter. The fluorescent reporter exhibits signal transition from 525 to 580 nm in the presence of unbound primers, and it correlates the binding affinity of label-free primers to the homozygous wild and mutant genomes. As a proof of concept, 26 real samples are studied relying on the ON and OFF fluorescence signals of the cationic polythiophene reporter. The results are analyzed by principal component analysis (PCA), which provides clear separation of healthy and patient individuals. The further analysis by support vector machine (SVM) classification has revealed that our assay converges to 96% overall accuracy. These results support that the PCR-free nucleic acid assay has a significant potential for rapid and cost-effective screening of familial Mediterranean fever.

KEYWORDS: *conjugated polyelectrolyte, PCR-free SNP detection, familial Mediterranean fever, DNA biosensors, nucleic acid assay*

Familial Mediterranean fever (FMF) is an autosomal recessive inherited disease and is common in ethnic origins such as Turks, Jews, Armenians, and Arabs.[1] The most prominent symptoms of the disease are periodic fever, joint and muscle pain, high erythrocyte sedimentation rate, and increased acute phase reactants such as C-reactive protein and fibrinogen.[2] Since the similar symptoms are common in several other diseases, diagnosis of FMF via routine hospital examinations is quite unlikely. Therefore, FMF diagnosis is only performed by genetic testing. Although there is no treatment to cure FMF, it is possible to suppress the symptoms and adverse effects of the disease by applying colchicine treatment. More importantly, diagnosis of FMF on time saves patients from severe kidney diseases in later stages.

The routine detection protocol of FMF is currently based on clinical symptoms, ethnicity, family history, and patient response to colchicine.[3] The Tel Hashomer criterion relying on classification of major and minor criteria is commonly used for high or low clinical suspicion and definitive diagnosis of FMF.[4] The major criterion is defined with the periodic fever accompanied by peritonitis, synovitis or pleuritis, and amyloidosis. FMF in first-degree relatives, erythema, and recurrent febrile episodes are the indicators of the minor Tel Hashomer criteria.[4,5] Determination of biallelic pathogenic variants of the *MEFV* gene by molecular genetic testing confirms the diagnosis. Although genetic testing can provide a definite diagnosis for FMF, it cannot be applied to all patients due to its high cost. So far, more than 70 mutations have been identified that cause FMF, and these are mostly seen in exon 10. The most prevalent mutations are M694V (32%), E148Q (20.6%), V726A (17%), and M680I (14.5%).[6] In a study, 8.41% of patients awaiting renal transplantation were found to be FMF patients.[7] Since kidney transplantation needs a suitable donor and is a costly approach, it is important to

Received: October 11, 2020
Accepted: February 1, 2021
Published: February 23, 2021

https://dx.doi.org/10.1021/acssensors.0c02130
ACS Sens. 2021, 6, 950–957

reduce this rate with early FMF diagnosis. Therefore, we propose that screening population for especially phenotype 2 FMF cases would reduce the renal failure rates and need for transplantation.

In recent years, conjugated polyelectrolytes have been utilized for detection of biological materials[8,9] such as proteins, nucleic acids, and small molecules and tissue/cell imaging.[10−13] One of the conjugated polyelectrolytes, polythiophenes (PT), has been widely studied in detection of biological materials because of the ability to switch between two basic conformations, "random coil and planar". The transition between these conformations is monitored by spectroscopic methods such as absorption and fluorescence spectroscopies.[14]

The numerous studies have well exploited the conformational change and concomitant optical transition for nucleic acid assays.[15−19] The basic detection mechanism relies on the interaction between cationic polythiophene (PT) and single-stranded DNA (ssDNA)/double-stranded DNA (dsDNA). When PT is introduced to ssDNA, an electrostatic interaction occurs, which results in a planar PT−ssDNA duplex. The planarization in PT increases the overlap of the π electrons and the effective conjugation length on the polymer backbone and hence changes the optical properties of PT.[20] The increased effective conjugation length on the backbone reduces the energy difference between the highest occupied molecular orbital (HOMO) and lowest unoccupied molecular orbital (LUMO) levels, which further causes a shift in absorbance toward the higher wavelengths (red) and quenching in fluorescence spectroscopy. In contrast to ssDNA, PT and dsDNA form a triplex complex by electrostatic interactions. In this case, the PT maintains its random coil conformation and spectroscopic properties are preserved, as well. Therefore, detection of alteration in the optical properties of PT by spectroscopic methods promotes the use of cationic polythiophene derivatives as DNA biosensors.[21] Utilizing conformational changes on the polythiophene backbone, there are many published studies related to the detection of biological materials, e.g., nucleic acids, proteins, and enzymes. Yildiz et al. developed a polythiophene-based fluorescence assay for determination of activity of ATPase by utilizing different conformational structures of the polythiophene backbone with coordination of adenosine 5'-triphosphate (ATP) and adenosine 5'-diphosphate (ADP).[22] As another study of ATP−polythiophene, they investigated ATP-dependent reactions by associating ATP-permeable polymer vesicles with a fluorescence polythiophene reporter.[23] The conformational changes on the polyelectrolyte backbone due to the energy bands provide a color switching, which is detectable even by the naked eye.[24−27] Yildiz et al. also developed a biosensor platform consisting of a cationic polythiophene derivative and polyvinylidene fluoride (PVDF) for the determination of the lung cancer-related miRNA sequence.[24] While the target miRNA with the cationic polythiophene and PNA triplex preserves the original color of the random coil polythiophene (orange), the noncomplementary sequence forms a duplex structure with polythiophene by electrostatic interactions and changes the color from orange to pink.

Detection of single-nucleotide polymorphism (SNP) is significant for diagnosis of diseases, especially genetic diseases. Therefore, many methods have been developed to detect SNPs on genomic DNA responsible for a certain disease. The well-known protocol for SNP detection is based on allele discrimination, which can be succeeded by primer extension, hybridization, ligation, and enzymatic cleavage methods.[28] These methods, however, require the polymerase chain reaction (PCR) protocol and specific enzymes, which are labor-intensive, time-consuming, and costly. Because of these drawbacks, PCR-free methodologies have been developed as alternative SNP detection methods.[29−35] These studies have overcome the PCR protocol; however, they still require complex steps like enzymatic reactions,[31,34] magnetic particle preparation,[29,35] and complexed chemical modifications.[32,33] The proposed method is based on hybridization of a small fragment DNA sequence (primer) to the complementary region on genomic DNA with a simple PCR and enzyme-free protocol. In this method, isolated genomic DNA is treated with wild-type (WT) and mutant-type (MT) primers separately at melting temperatures of primers. After that, genomic DNA is precipitated and supernatants are collected for fluorescence analysis with a cationic polythiophene (PT) derivative. If the genomic DNA is homozygous wild (HZW), the wild-type complementary primer is more efficiently associated with genomic DNA. On the other hand, a mutant-type noncomplementary primer cannot hybridize to homozygous wild-type genomic DNA. From these two collected supernatants, therefore, the former is poor in wild-type primers and the latter is rich in mutant-type primers. Consequently, the latter can cause significant conformational change in the PT backbone, thereupon inducing optical transition in the fluorescence spectrum. Familial Mediterranean fever (FMF) was chosen as a model genetic disease to detect single-nucleotide polymorphism. Pathogenic M694V variation of the *MEFV* gene is the most common and widely studied mutation in FMF clinics. M694V mutation is caused by the A/G single-nucleotide transition. The proposed methodology may lead to facilitate screening of samples prior to analysis and may provide quick separation of healthy individuals prior to the PCR analysis process, thereby saving costs in FMF detection.

EXPERIMENTAL SECTION

Materials. All reagents were purchased from Sigma Aldrich and used without further purification. Twenty nine base pair oligonucleotides of wild and mutant types were synthesized and purchased from OLIGOMER (Turkey). Human anonymized genome samples were provided by Dokuz Eylul University, Department of Medical Genetics, Faculty of Medicine. The study was approved by the local ethics committee.

Synthesis of Cationic Polyelectrolyte. *Synthesis of 3-Methoxy-4-methylthiophene (Precursor 1, PC1).* 1-Methyl-2-pyrolidinone (1 mL) and 25 wt % freshly synthesized sodium methoxide (0.479 g, 8.85 mmol) are mixed in a round-bottom flask. Sodium methoxide (25 wt %) was synthesized from sodium metal and dry methanol. 3-Bromo-4-methylthiophene (0.5 g, 2.82 mmol) and CuBr (0.25 g, 1.74 mmol) were added into the mixture and then reflux at 110 °C for 3 days. After the reaction mixture was cooled down to room temperature, 0.1 g of sodium bromide in 4 mL of deionized (DI) water was added and stirred at room temperature for an hour. The mixture was extracted with 10 mL of diethyl ether 4−5 times. During extraction, the organic phase was washed with DI water and dried over $MgSO_4$. The solvent was removed by a rotary evaporator to yield a light yellow oil. The product was purified by column chromatography to yield 3-methoxy-4-methylthiophene (PC1, 90%). ^{1}H NMR (400 MHz, $CDCl_3$) δ (ppm): 6.82 (1H, d), 6.16 (1H, d), 3.82 (3H, s), 2.10 (3H, s).

Synthesis of 3(3-Bromo)propoxy-4-methylthiophene (Precursor 2, PC2). 3-Methoxy-4-methylthiophene (100 mg, 0.78 mmol), 3-bromo-1-propanol (150 μL, 1.66 mmol), $NaHSO_4$ (12.5 mg, 0.1 mmol), and 2 mL of toluene were mixed in a round-bottom flask. The

https://dx.doi.org/10.1021/acssensors.0c02130
ACS Sens. 2021, 6, 950−957

reaction medium was heated to 100 °C for 1 day under a N_2 atmosphere. After the reaction mixture was cooled down to room temperature, toluene was evaporated. The mixture was then extracted with diethyl ether 4−5 times, washed with DI water, and dried over $MgSO_4$. Diethyl ether was removed by a rotary evaporator, and the crude product was purified by column chromatography to yield 3(3-bromo)propoxy-4-methylthiophene (PC2, 85%) as a colorless oil. ^{1}H NMR (400 MHz, $CDCl_3$) δ (ppm): 6.84 (1H, d), 6.18 (1H, d), 4.09 (2H, t), 3.61 (2H, t), 2.34 (2H, p), 2.09 (3H, s).

Synthesis of Monomer N-Allyl-N-methyl-N-(3-((4-methylthiophen-3-yl)oxy)propyl)prop-2-en-1-aminium Bromide. PC2 (60 mg, 0.26 mmol), diallylmethylamine (704 μL, 5.0 mmol), and 2.5 mL of tetrahydrofuran (THF) were added into a round-bottom flask and stirred at 72 °C for 48 h. The reaction mixture was cooled down to room temperature and then transferred to a 15 mL centrifuge tube. The mixture was centrifuged at 3000 rpm for 5 min, and the supernatant was removed. The precipitate was washed with THF and centrifuged again. This process was repeated several times, and the final precipitate (monomer, 67%) was dried under vacuum. ^{1}H NMR (400 MHz, D_2O) δ (ppm): 6.90 (1H, d), 6.36 (1H, d), 5.89 (2H, ddt), 5.57 (4H, dt), 4.02 (2H, t), 3.80 (4H, m), 3.30 (2H, t), 2.89 (3H, s), 2.17 (2H, p), 1.95 (3H, s).

Synthesis of Cationic Polyelectrolyte Poly(N-allyl-N-methyl-N-(3-((4-methylthiophen-3-yl)oxy)propyl)prop-2-en-1-aminium Bromide). $FeCl_3$ (60 mg, 0.38 mmol) was dissolved in 2.3 mL of $CHCl_3$ and then added dropwise to the monomer (30 mg, 0.11 mmol) solution dissolved in 1.5 mL of $CHCl_3$. The mixture was stirred at room temperature for 1 day under a N_2 atmosphere. The reaction mixture was washed with $CHCl_3$ and centrifuged at 4000 rpm for 5 min. The dark green precipitate was dried under vacuum. The NMR characterization (400 MHz) for the polymer was performed in D_2O (2 mg/mL). The typical NMR spectrum of the polymer yielded broadened peaks at around 5.70, 5.40, 3.67, 2.75, and 1.94 ppm (shown in Figure 1a with dashed lines).

Isolation of Human Genome. Anonymized FMF patient samples from the DNA bank of Dokuz Eylul University, Faculty of Medicine, Department of Medical Genetics, were used as a genomic DNA source. Samples stored at −80 °C were isolated according to the manufacturer's procedure using the "High Pure PCR Template isolation (Roche)" kit. The DNAs obtained were measured using the "Nanodrop (Thermo)" instrument, and the concentration and purity of the samples were determined by measuring their absorbance at 260 and 280 nm wavelengths. The concentrations of isolated samples, which were analyzed in this study, were recorded within the range of around 10 and 70 ng/μL. The average concentration of homozygous wild (HZW) samples was 43.96 ng/μL and that of homozygous mutant and heterozygous samples (HZM and HTZ) was 46.17 ng/μL. To design wild-type and mutant primers, sequence data of the *MEFV* gene were obtained from NCBI and Ensembl databases for Human and designed using the "primer3" program. The specificity of the designed primers was checked using Blast and UCSC in silico PCR software programs.

Detection of M694V SNP Using Real-Time PCR. The DNAs obtained were studied in accordance with the procedure in the LightCycler FastStart DNA Master Hyb Probe (Roche) kit specific to the LightSNiP FMF M694V (rs61752717) gene and SNPs.

LightSNiP FMF M694V (rs61752717) mutation was identified as wild type, heterozygous, and mutant using the melting curve analysis method in LC480 software.

Primers' and Probes' Design. The reference sequences of *MEFV* gene and rs61752717, also known as c.2080A>G, p.Met694Val or M694V which is an SNP in the *MEFV* gene, were downloaded from NCBI (http://www.ncbi.nlm.nih.gov/) and "dbSNP Short Genetic Variations" database, respectively. Multiple sequence alignment was performed using the Clustal Omega algorithm in EMBL-EBI (www.ebi.ac.uk). LightCycler Probe Design Software 2.0 (version 2.0; Roche) was used to design the primers and probe for M694V SNP in the *MEFV* gene.

Sequences of primers and probe:

F: 5′-TCATCATTATCACCACCCAGTAGCC-3′.

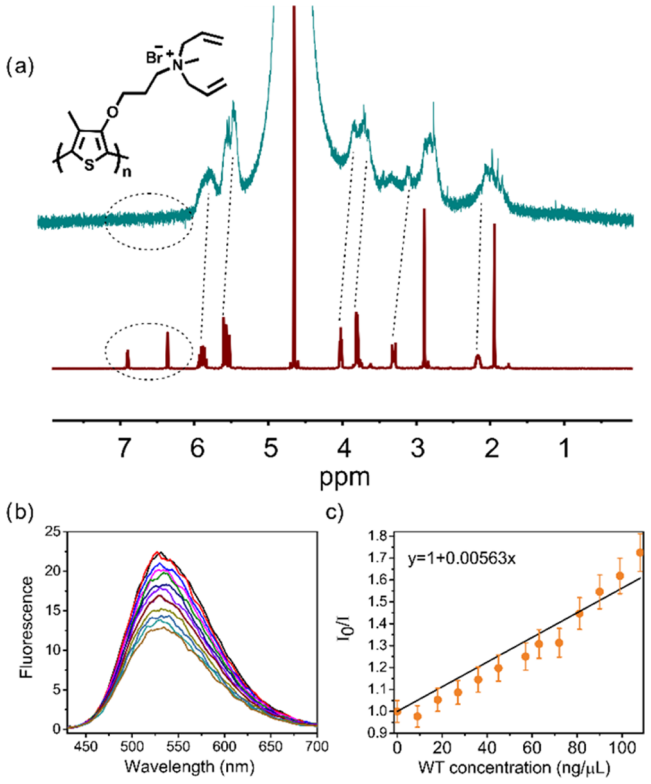

Figure 1. (a) 1H NMR spectra of PT and its monomer. The inset is the chemical structure of the cationic polythiophene (PT) reporter. (b) Fluorescence titration spectra of PT (1.8 mM of 200 μL) with WT from the concentration of 0 (top) to 108 ng/μL (bottom). (c) Stern−Volmer plot of (b).

R: 3′-GAGCCTGCAAGACATCC-5′.

Sprob:5′-Fluorescein-SPC-GGCTACTGGGTGGTGATAATGATGA-Phosphate-3′.

Hybridization Protocol. The isolated genomic DNAs were treated with wild- and mutant-type primers of the *MFEV* gene separately, and their sequences are as follows:

Wild-type primer:

TGATAATGATGAAGGAAAATGAGTACCAG.

Mutant-type primer:

TGATAATGGTGAAGGAAAATGAGTACCAG.

The genomic DNA and primer mixtures were heated to 95 °C for 1 h to denature the genomic DNA strands. The mixtures were then incubated at 61 and 62 °C (the melting temperatures of primers) for 2 h for the hybridization step of wild-type (WT) and mutant-type (MT) primers, respectively. After incubation, the complementary primer hybridizes to the genomic DNA and the noncomplementary primer does not hybridize (or does hybridize in trace amount). Immediately, the mixtures were centrifuged at 10 000 rpm for 30 min to precipitate genomic DNA and then supernatants were carefully collected.

Optical Characterization. Absorption spectra were recorded using a Schimadzu UV 2550 spectrophotometer. A quartz cuvette with 0.1 cm optical path length and 1 cm width (Hellma) was used in absorption analysis. Steady-state fluorescence spectra were recorded using a Thermo Scientific Varioskan Flash microplate reader with 384-well black plates. Fluorescence emission spectra were measured with excitation at maximum absorption wavelength.

Fluorescence Analysis of DNA Solutions. After the hybridization protocol, the DNA solutions were analyzed with polythiophene solutions by fluorescence spectroscopy. The PT solution (10 μL, 0.5 mg/mL) was first diluted to 20 μL with Tris-ethylenediaminetetraacetic acid (EDTA) buffer (TE). Then, 2 μL of rWT and rMT solutions was added to PT solutions, and the PT-

https://dx.doi.org/10.1021/acssensors.0c02130
ACS Sens. 2021, 6, 950−957

Scheme 1. PCR-Free Assay for Detection of Single-Nucleotide Polymorphism by a Cationic Polyelectrolyte[a]

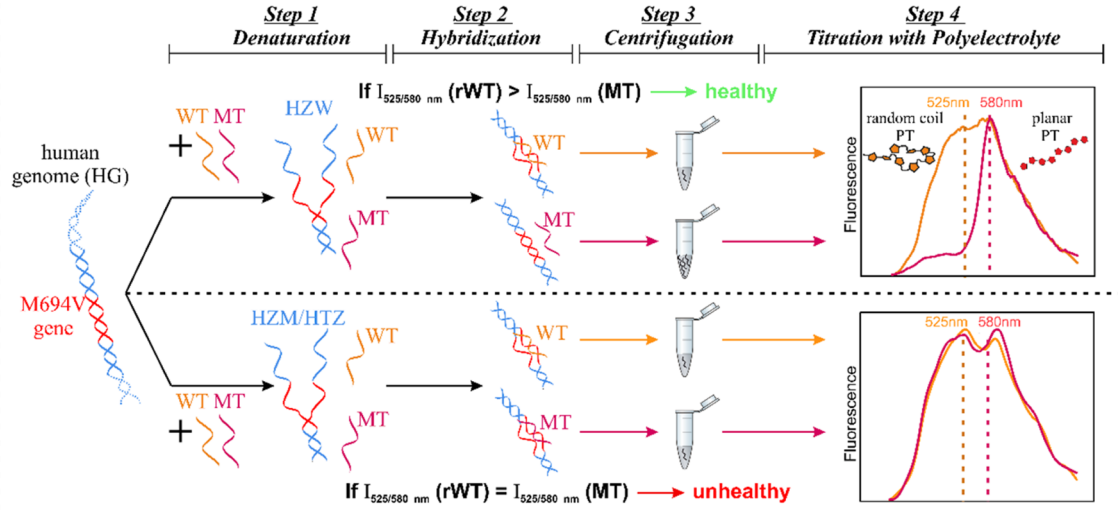

[a]HG, human genome; WT, wild-type primer; MT, mutant-type primer; HZW, homozygous wild-type human genome; HZM, homozygous mutant-type human genome; HTZ, heterozygous human genome.

DNA solutions were gently vortexed before adding them to the well plate.

RESULTS AND DISCUSSION

Scheme 1 illustrates the four-step PCR-free methodology for detection of FMF-associated single-nucleotide polymorphism (SNP). In the first step, typically 30 μL of the DNA extract of the clinical sample stored in the Tris-EDTA (TE) buffer is split into two equivolume solutions as solution A and solution B for the denaturation of genomic DNAs. The special design wild-type (WT) and mutant-type (MT) pseudoprimers are then added into solution A and solution B, respectively, prior to the annealing process. At step two, solutions are annealed and incubated at the melting temperature of each primer for the hybridization process followed by a quick centrifugation to separate unhybridized remaining primers. The supernatants from solution A (containing remaining WT) and from solution B (containing remaining MT), which are hereinafter referred to as rWT and rMT, respectively, are collected for spectrometric measurements at the final step. Depending on the hybridization efficiency of WT and MT with target genes of homozygous wild (HZW, healthy subjects), homozygous mutant (HZM, patients), and heterozygous (HTZ, carrier), the final amount of rWT and rMT differs in supernatant solutions. Since the fluorescent reporter PT is bearing cationic charges, rWT and rMT are prone to form rWT−PT and rMT−PT complexes that cause transition in fluorescence from 525 to 580 nm. The yield of fluorescence transition is found to be proportional to the unhybridized extent of pseudoprimers, and this facilitates SNP detection without PCR multiplication. We use a simple algorithm that compares the fluorescence intensities (I_{525} and I_{580}) between rWT−PT and rMT−PT and is operated for final decision of clinical samples. The logic is given as follows:1. If rWT $I_{525/580}$ > rMT $I_{525/580}$, then the subject is healthy (HZW);

2. If rWT $I_{525/580}$ = rMT $I_{525/580}$, then the subject is unhealthy (HZM or HTZ).

Figure 1a inset shows the chemical structure of the fluorescent reporter PT poly(*N*-allyl-*N*-methyl-*N*-(3-((4-methylthiophen-3-yl)oxy)propyl)prop-2-en-1-aminium bromide). The NMR spectra of the monomer and polymer have been shown in Figure 1a satisfying the structures (peak assignments were given in the experimental part). Figure 1b shows the WT concentration-dependent fluorescence response of PT. As the concentration increases from 10 to 70 ng/μL (relevant to the clinical concentration of genomic DNA), the fluorescence intensity quenches. Emission intensities at the maximum wavelength of fluorescence titration curves in Figure 1b were utilized for the Stern−Volmer plot (I_0/I) displayed in Figure 1c. Using Origin 9 software, linear least-squares regression between WT concentrations and I_0/I was applied. The *R*-square of the resulting linear line was calculated as 0.997, and the slope used was 0.00563. The calibration curve in Figure 1c reveals the linear correlation of fluorescence intensity to increasing pseudoprimer concentration. This correlation assures that rWT and rMT are detectable by monitoring the fluorescence signal of PT.

The proposed algorithm has been validated for 26 clinical samples. It has accomplished classification of separate groups in 26 samples. Twelve samples (given in Figure 2) were found to be exhibiting high affinity to pseudoprimer WT, while the rest 14 samples were prone to associate with pseudoprimer MT (given in Figure 3).

Figure 2a shows WT and MT sequences and illustrates the probable hybridization pattern. Here, the MT sequence is expected to remain unbound or the rMT concentration is higher than that of rWT in final supernatant solutions. Figure 2b shows the fluorescence intensity profile of 12 clinical samples after the proposed assay was applied. The orange bars show the intensity profile of the rWT−PT complex, while pink bars are rMT−PT complexes. If the genomic DNA has the wild-type sequence on the *MEFV* gene region, the then WT pseudoprimer (complementary) has to hybridize to genomic DNA more efficiently than the MT pseudoprimer (non-complementary). Since rWT is in trace amounts in the final supernatant solution, it does not quench PT emission at 525 nm. However, rMT is abundant in the supernatant solution since it does not hybridize efficiently; therefore, it causes significant fluorescence quenching in PT at 525 nm. As illustrated in Figure 2, fluorescence intensity of rWT−PT is

https://dx.doi.org/10.1021/acssensors.0c02130
ACS Sens. 2021, 6, 950−957

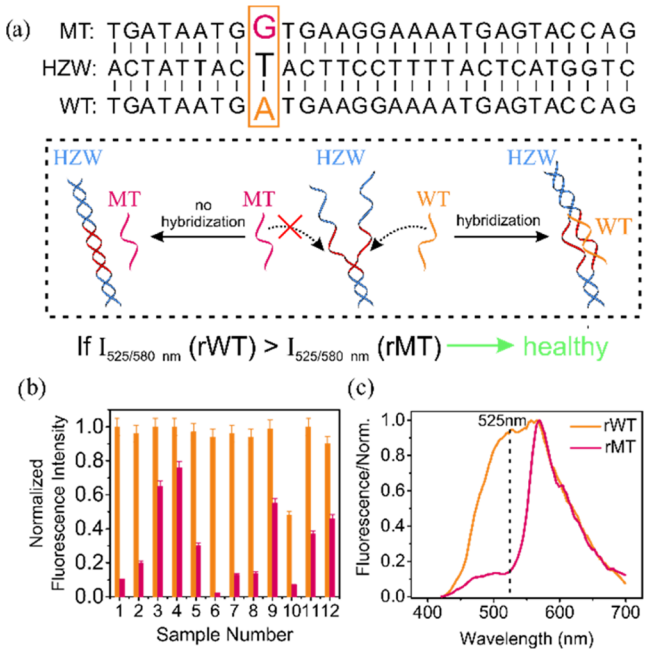

Figure 2. (a) Schematic representation of the hybridization protocol for HZW samples. (b) Fluorescence intensity comparison at 525 nm of the PT−rWT complex (orange) and PT−rMT complex (pink). (c) Fluorescence spectra of sample 8 (20 μL of 0.9 mM PT solution used in fluorescence analysis).

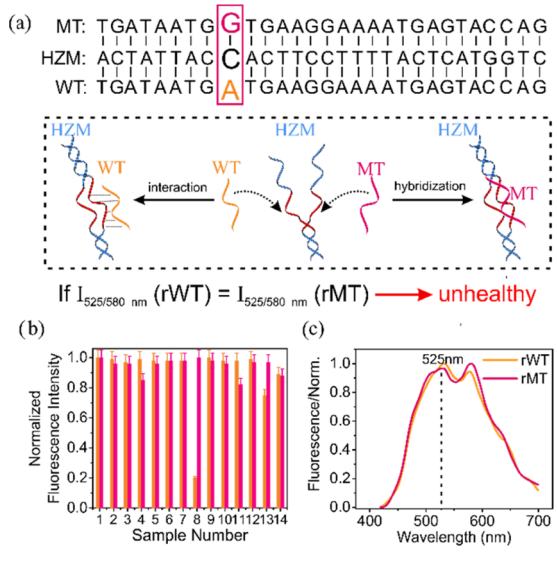

Figure 3. (a) Schematic representation of the hybridization protocol for HZM samples. (b) Fluorescence intensity at 525 nm of the PT−rWT complex (orange) and PT−rMT complex (pink). (c) Fluorescence spectra of sample 5 (20 μL of 0.9 mM PT solution used in fluorescence analysis).

nearly 3 times greater than that of rMT−PT. In this analysis, 12 human DNA samples are utilized, and the same behavior is observed for each sample. Based on the proposed algorithm, these intensity profiles refer to healthy subjects; therefore, the algorithm classifies 12 of 26 samples as HZW [homozygous wild-type isolated human genomes]. Figure 2c shows the typical fluorescence spectrum of random coil (orange trace) and planar conformations (pink trace) referring to rWT−PT and rMT−PT, respectively. The peak at 580 nm is assigned as a lower energy peak due to the planarized form of polymer PT; however, it is observable at a lower PT concentration (PT < 1.2 mM); otherwise, it is concealed (see Figure 1b for higher concentration response).

Figure 3a shows the pseudoprimer MT and HZM sequence and illustrates the probable binding motif. Figure 3b shows the rest 14 samples' fluorescence intensity profile, indicating the rMT−PT complex exhibiting strong fluorescence at 525 nm. This profile refers to MT binding to the genomic DNA that has the mutant-type sequence on the *MEFV* gene mutation region. For the 14 samples, the MT pseudoprimer (complementary) hybridizes to genomic DNA.

The assay methodology classifies two groups in 26 samples referring to homozygous wild (HZW) and homozygous mutant (HZM) or heterozygous (HTZ). To validate the capability of the proposed assay, we have performed qPCR measurements for 26 samples. We have used the primers and SimpleProbe probes specific for *MEFV* (FMF) genes to allow the detection of single-nucleotide polymorphism (SNP of M694V) in DNA samples using melting curve analysis after real-time PCR reactions. Here, SimpleProbe is a single probe containing the SNP site labeled with a quencher and fluorescein at the 5′-end. This probe is designed to specifically hybridize to a target sequence that contains the SNP of M694V. qPCR instruments can detect melting of the probe−target hybrids as the temperature increases. The more stable the hybridization between SimpleProbe and the wild-type sequence, the higher the melting temperature. Mutations like V694V SNPs weaken the stability of SimpleProbe binding, and we can observe the peaks at low temperatures.

Figure 4 shows the fluorescence versus temperature curve (melting curve) of each variation in the MEFV gene. In each

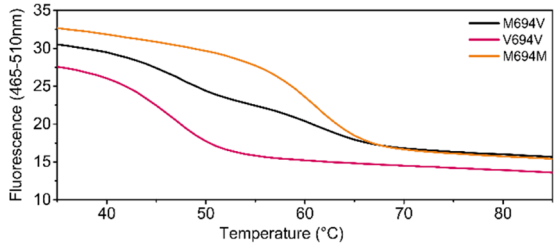

Figure 4. Melting curve of the *MEFV* gene variations: M694V-heterozygous, V694V-homozygous mutant, and M694M-homozygous wild.

sample, the fluorescence signal clearly decreases as the temperature increases, which is reflecting the quenching of the SimpleProbe signal as the probe is displaced from its target. Twelve samples among 26 exhibit melting transition at a slightly higher temperature (orange curve) as compared to the other samples. The first negative derivative of the fluorescence signal shown in Figure 5 indicates melting temperature at 61 °C for M694M-homozygous wild (HZW). The rest of the 14 samples exhibit single-step melting transitions at 55 °C (7 patients, V694V) and double-step transitions both at 55 and 61 °C (7 carriers, M694V). The higher melting temperature of homozygous wild samples is attributed to the perfect match between the M694M sequence and probe as compared to homozygous mutant samples (lower melting peak that reflects the sequence mismatches between the V694V sequence and probe). The qPCR results assure that homozygous (12:HZW) and homozygous mutant + heterozygous (14:HZM + HZT) samples are perfectly correlated with the proposed assay. This

https://dx.doi.org/10.1021/acssensors.0c02130
ACS Sens. 2021, 6, 950−957

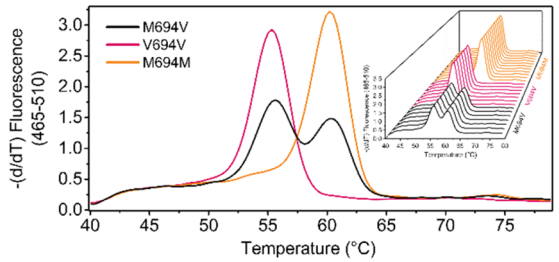

Figure 5. Real-time PCR results indicating the melting temperatures of *MEFV* gene variations (M694V, V694V, and M694M). The inset figure represents the data of total 26 genomic DNA studied in this work.

result assures that the proposed methodology is able to differentiate healthy subjects with 100% precision from patients and carriers. Moreover, the differentiation of HZW (healthy) and HZM + HTZ (patients + carriers) is found to be as accurate as PCR.

We further analyzed the fluorescence signals by applying data analysis techniques to standardize the methodology. First, PCA was applied to fluorescence intensities at two wavelengths for both rWT−PT and rMT−PT complexes (four variables for each sample). PCA provides reduced number of dimensions by projecting multivariate data to orthogonal directions, which maximize the variance. In other words, PCA allows interpretable visualization and reveals underlying patterns within the multivariate data set in a robust manner. By PCA, each sample with these four aforementioned variables was projected to a new two-dimensional score space consisting of first two principal components, namely, PC1 and PC2, where each point represents a single sample. PC1 and PC2 accounted for 96.31% of total variance in the data set where individual explained variances were 76.39 and 19.92% for PC1 and PC2, respectively. While visual evaluation of the score plot showed a clear separation of homozygous wild (HZW) and homozygous mutant (HZM)−heterozygous (HTZ) samples, PCA alone as an unsupervised method cannot provide a mathematical classification method; thus, support vector machine (SVM) classification was applied to PCA scores (only to PC1 and PC2), and an optimal linear decision boundary was obtained. The entire procedure was carried out in a Python 3 environment, and scikit-learn[36] library was utilized for data analysis. The combined results of the PCA+SVM approach are shown in Figure 6. Of 26 samples (12 HZW, 14 HZM + HTZ), only a single sample belonging to HZW was misclassified by a small margin, yielding an overall classification accuracy of 96%. Moreover, given that the mutant class is referred to as the positive class, the sensitivity and specificity of the model were calculated as 100 and 92%, respectively. From Figure 6, it is also clear that the first PC is the main axis of separation where the most HZW samples are clustered on the right side of PC1 and HZM−HTZ samples are on the left side. Hence, the PCA loadings of PC1, which is the vector used for projection of the data to the first PC, were utilized to assign relative variable importance. In Figure 7, a bar graph of PC1 loadings is given, and it shows that the loading corresponding to the fluorescence reading of PT that is complexed with the mutant-type primer-treated human genome samples at 525 nm has a significantly greater absolute value and may be considered as the most influencing variable for both the separation at PC1 and the success of the classification. The

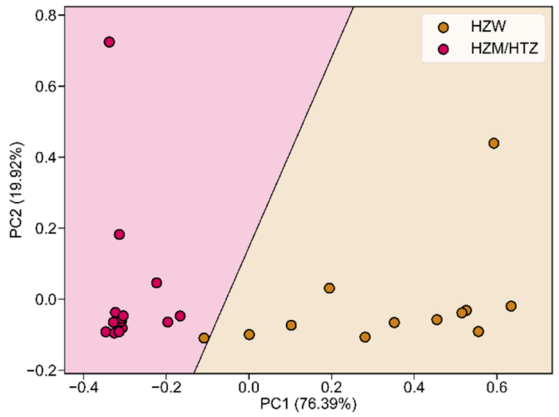

Figure 6. Two-dimensional (2D) PCA scores of all samples along with the decision boundary obtained by SVM classification.

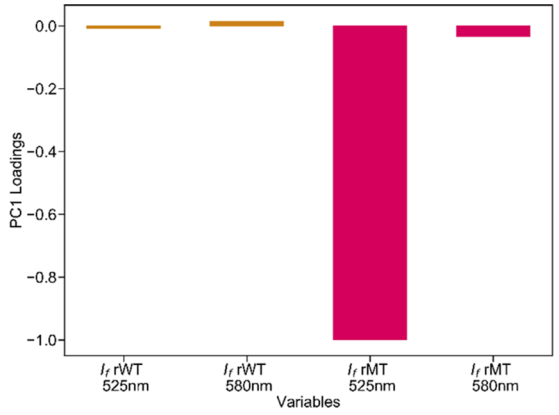

Figure 7. Loadings' plot for PC1.

results assure that HZW and HZM−HTZ are classified by the proposed algorithm and the assay is validated.

CONCLUSIONS

This study demonstrates a 4-step and PCR-free protocol for SNP detection with a cationic conjugated polyelectrolyte. The fluorescent reporter "PT" that is sensitive to the amount of unhybridized pseudoprimer is utilized to monitor the fluorescence intensity difference between rWT and rMT. The results reveal that SNP detection on FMF-related gene regions is achieved in the range of clinical concentration of genomic DNA (10−70 ng/μL). The data analysis of the fluorescence spectra (525 and 580 nm) is carried out using PCA followed by SVM for the classification of HZW and HZM/HTZ genomic DNA samples and provides 96% accuracy. Additionally, the cost for proposed methodology is less than $1.5, which is significantly lower than the estimated cost of FMF (genetic disease associated with SNP) tests, about $15−70 per patient (cost analysis, advantages, and limitations of commercial tests for FMF are given in Table 1). The use of proposed screening methodology might provide advantage in separation of healthy individuals from samples in high volume and eliminate the further PCR testing steps and therefore saving cost. The proposed protocol has a great potential to differentiate healthy individuals from the FMF patients with a simple and rapid fluorescence analysis. Overall, our PCR-free nucleic acid assay has a significant potential for rapid and cost-effective screening of familial Mediterranean fever. PCR is a

https://dx.doi.org/10.1021/acssensors.0c02130
ACS Sens. 2021, 6, 950−957

Table 1. List of Some FMF Diagnosis Methods with Their Cost and Time in the Literature and Web Catalogue of Companies

method	test	company	cost per test	time	references or catalogue no
minisequencing	MEFV	labistanbul	~$70	N/A	37
	MEFV	N/A	~$71	N/A	38
nextGen sequencing	MEFV	prevention genetics	$640	avg. 18 days	39
PCR	MEFV	Anatolia	$14.5	~1−2 h	ABFMF7
PCR	MEFV	Tibmolbiol	$26.6	~1−2 h	07147481001
PCR	MEFV	Zena Dia	$23	~1−2 h	KD6466292-100
PCR	MEFV	Bioactiva	$15	~1−2 h	BA481
prescreening	MEFV	present study	~$1.5[a]	~3 h	present study

[a]The cost of test was calculated for the production of 1 g of polymer and 100 ng of primers of each; 1 g/L polymer solution is sufficient for 1000 test kits.

golden standard method, and our assay promises a potential pre-evaluation step in the overall detection process; therefore, it may find potential application together with the PCR technique.

■ ASSOCIATED CONTENT

Supporting Information

The Supporting Information is available free of charge at https://pubs.acs.org/doi/10.1021/acssensors.0c02130.

NMR spectra for each synthesis step of the cationic polyelectrolyte; concentrations of genomic DNAs utilized in this study; isolation of human genome; the whole real-time PCR protocol; further information regarding the data analysis and performance evaluations along with the complete Python script (PDF)

■ AUTHOR INFORMATION

Corresponding Authors

Altug Koc − *Department of Medical Genetics, Faculty of Medicine, Dokuz Eylul University, Izmir 35330, Turkey*; Email: draltugkoc@gmail.com

Umit Hakan Yildiz − *Department of Chemistry and Department of Photonic Science and Engineering, Izmir Institute of Technology, İzmir 35430, Turkey*; orcid.org/0000-0002-6922-4454; Email: hakanyildiz@iyte.edu.tr

Authors

Muge Yucel − *Department of Bioengineering and Biotechnology, Izmir Institute of Technology, Izmir 35430, Turkey*; orcid.org/0000-0001-7032-392X

Ayfer Ulgenalp − *Department of Medical Genetics, Faculty of Medicine, Dokuz Eylul University, Izmir 35330, Turkey*

Gun Deniz Akkoc − *Department of Chemistry, Izmir Institute of Technology, İzmir 35430, Turkey*

Metin Ceyhan − *Department of Basic Oncology, Institute of Oncology, Dokuz Eylul University, Izmir 35330, Turkey*

Complete contact information is available at: https://pubs.acs.org/10.1021/acssensors.0c02130

Notes

The authors declare no competing financial interest.

■ ACKNOWLEDGMENTS

This research has been supported by a grant from the Scientific and Technological Research Council of Turkey, TUBİTAK (Grant No: 116Z547). We are thankful for financial support of İzmir Institute of Technology Scientific Project Fund (IYTE BAP-291). Authors M.Y. and G.D.A. are YÖK 100-2000 scholarship holders.

■ REFERENCES

(1) Livneh, A.; Langevitz, P. Diagnostic and treatment concerns in familial Mediterranean fever. *Best Pract. Res., Clin. Rheumatol.* **2000**, *14*, 477−498.

(2) El-Shanti, H. Familial Mediterranean Fever and Renal Disease. *Saudi J. Kidney Dis. Transplant.* **2003**, *14*, 378−385.

(3) Settin, A.; El-Baz, R.; Abd Rasool, M.; El-Khalegy, H.; El-Sayed, O.; El-Bendary, M.; Al-Nagar, A.-S. M. Clinical and molecular diagnosis of Familial Mediterranean Fever in Egyptian children. *J. Gastrointest. Liver Dis.* **2007**, *16*, 141−145.

(4) Samli, H. D. O.; Bukulmez, A.; Yuksel, E.; Ovali, F.; Solak, M. Relationship of Tel Hashomer criteria and Mediterranean fever gene mutations in a cohort of Turkish familial Mediterranean fever patients. *Saudi Med. J.* **2006**, *27*, 1822−1826.

(5) Livneh, A. L. P.; Zemer, D.; Zaks, N.; Kees, S.; Lidar, T.; Migdal, A.; Padeh, S.; Pras, M. Criteri for the Diagnosi of Familial Mediterranean Fever. *Arthritis Rheum.* **1997**, *40*, 1879−1885.

(6) Caglayan, A. O.; Demiryilmaz, F.; Ozyazgan, I.; Gumus, H. MEFV gene compound heterozygous mutations in familial Mediterranean fever phenotype: a retrospective clinical and molecular study. *Nephrol., Dial., Transplant.* **2010**, *25*, 2520−2523.

(7) Keles, M.; Eyerci, N.; Uyanik, A.; Aydinli, B.; Sahin, G. Z.; Cetinkaya, R.; Pirim, I.; Polat, K. Y. The frequency of familial mediterranean Fever related amyloidosis in renal waiting list for transplantation. *Eurasian J. Med.* **2010**, *42*, 19−20.

(8) Nilsson, K. P. R.; Inganäs, O. Chip and solution detection of DNA hybridization using a luminescent zwitterionic polythiophene derivative. *Nat. Mater.* **2003**, *2*, 419−424.

(9) Yeasmin, S.; Ammanath, G.; Ali, Y.; Boehm, B. O.; Yildiz, U. H.; Palaniappan, A.; Liedberg, B. Colorimetric Urinalysis for On-site Detection of Metabolic Biomarkers. *ACS Appl. Mater. Interfaces* **2020**, *12*, 31270−31281.

(10) Wu, C.; Szymanski, C.; Cain, Z.; McNeill, J. Conjugated Polymer Dots for Multiphoton Fluorescence Imaging. *J. Am. Chem. Soc.* **2007**, *129*, 12904−12905.

(11) Ye, F.; Wu, C.; Jin, Y.; Wang, M.; Chan, Y.-H.; Yu, J.; Sun, W.; Hayden, S.; Chiu, D. T. A compact and highly fluorescent orange-emitting polymer dot for specific subcellular imaging. *Chem. Commun.* **2012**, *48*, 1778−1780.

(12) Yu, J.; Rong, Y.; Kuo, C.-T.; Zhou, X.-H.; Chiu, D. T. Recent Advances in the Development of Highly Luminescent Semiconducting Polymer Dots and Nanoparticles for Biological Imaging and Medicine. *Anal. Chem.* **2017**, *89*, 42−56.

(13) Özenler, S.; Yucel, M.; Tüncel, Ö.; Kaya, H.; Özçelik, S.; Yildiz, U. H. Single Chain Cationic Polymer Dot as a Fluorescent Probe for Cell Imaging and Selective Determination of Hepatocellular Carcinoma Cells. *Anal. Chem.* **2019**, *91*, 10357−10360.

(14) Garreau, S.; Leclerc, M.; Errien, N.; Louarn, G. Planar-to-Nonplanar Conformational Transition in Thermochromic Polythiophenes: A Spectroscopic Study. *Macromolecules* **2003**, *36*, 692−697.

(15) Ho, H.-A.; Boissinot, M.; Bergeron, M. G.; Corbeil, G.; Doré, K.; Boudreau, D.; Leclerc, M. Colorimetric and Fluorometric Detection of Nucleic Acids Using Cationic Polythiophene Derivatives. *Angew. Chem., Int. Ed.* **2002**, *41*, 1548−1551.
(16) Ho, H.-A.; Béra-Abérem, M.; Leclerc, M. Optical Sensors Based on Hybrid DNA/Conjugated Polymer Complexes. *Chem. - Eur. J.* **2005**, *11*, 1718−1724.
(17) He, F.; Feng, F.; Duan, X.; Wang, S.; Li, Y.; Zhu, D. Selective and Homogeneous Fluorescent DNA Detection by Target-Induced Strand Displacement Using Cationic Conjugated Polyelectrolytes. *Anal. Chem.* **2008**, *80*, 2239−2243.
(18) Xia, F.; Zuo, X.; Yang, R.; Xiao, Y.; Kang, D.; Vallée-Bélisle, A.; Gong, X.; Yuen, J. D.; Hsu, B. B. Y.; Heeger, A. J.; Plaxco, K. W. Colorimetric detection of DNA, small molecules, proteins, and ions using unmodified gold nanoparticles and conjugated polyelectrolytes. *Proc. Natl. Acad. Sci. U.S.A.* **2010**, *107*, 10837−10841.
(19) Liang, J.; Li, K.; Liu, B. Visual sensing with conjugated polyelectrolytes. *Chem. Sci.* **2013**, *4*, 1377−1394.
(20) Ho, H.-A.; Najari, A.; Leclerc, M. Optical Detection of DNA and Proteins with Cationic Polythiophenes. *Acc. Chem. Res.* **2008**, *41*, 168−178.
(21) Feng, X.; Liu, L.; Wang, S.; Zhu, D. Water-soluble fluorescent conjugated polymers and their interactions with biomacromolecules for sensitive biosensors. *Chem. Soc. Rev.* **2010**, *39*, 2411−2419.
(22) Yildiz, U. H.; Sheng, C. W.; Mailepessov, D.; Xueqi, D. C.; Shochat, S. G.; Liedberg, B. Real-time determination of the activity of ATPase by use of a water-soluble polythiophene. *Anal. Bioanal. Chem.* **2012**, *404*, 2369−2375.
(23) Yildiz, U. H.; De Hoog, H.-P. M.; Fu, Z.; Tomczak, N.; Parikh, A. N.; Nallani, M.; Liedberg, B. Third-Party ATP Sensing in Polymersomes: A Label-Free Assay of Enzyme Reactions in Vesicular Compartments. *Small* **2014**, *10*, 442−447.
(24) Yildiz, U. H.; Alagappan, P.; Liedberg, B. Naked Eye Detection of Lung Cancer Associated miRNA by Paper Based Biosensing Platform. *Anal. Chem.* **2013**, *85*, 820−824.
(25) Rajwar, D.; Ammanath, G.; Cheema, J. A.; Palaniappan, A.; Yildiz, U. H.; Liedberg, B. Tailoring Conformation-Induced Chromism of Polythiophene Copolymers for Nucleic Acid Assay at Resource Limited Settings. *ACS Appl. Mater. Interfaces* **2016**, *8*, 8349−8357.
(26) Ammanath, G.; Yeasmin, S.; Srinivasulu, Y.; Vats, M.; Cheema, J. A.; Nabilah, F.; Srivastava, R.; Yildiz, U. H.; Alagappan, P.; Liedberg, B. Flow-through colorimetric assay for detection of nucleic acids in plasma. *Anal. Chim. Acta* **2019**, *1066*, 102−111.
(27) Aydın, H. B.; Cheema, J. A.; Ammanath, G.; Toklucu, C.; Yucel, M.; Özenler, S.; Palaniappan, A.; Liedberg, B.; Yildiz, U. H. Pixelated colorimetric nucleic acid assay. *Talanta* **2020**, *209*, No. 120581.
(28) Sukhumsirichart, W. Polymorphisms. In *Genetic Diversity and Disease Susceptibility*; IntechOpen, 2018.
(29) Dubus, S.; Gravel, J.-F.; Le Drogoff, B.; Nobert, P.; Veres, T.; Boudreau, D. PCR-Free DNA Detection Using a Magnetic Bead-Supported Polymeric Transducer and Microelectromagnetic Traps. *Anal. Chem.* **2006**, *78*, 4457−4464.
(30) Duan, X.; Liu, L.; Feng, F.; Wang, S. Cationic Conjugated Polymers for Optical Detection of DNA Methylation, Lesions, and Single Nucleotide Polymorphisms. *Acc. Chem. Res.* **2010**, *43*, 260−270.
(31) Kim, J. H. PCR free multiple ligase reactions and probe cleavages for the SNP detection of KRAS mutation with attomole sensitivity. *Analyst* **2016**, *141*, 6381−6386.
(32) Pei, H.; Lu, N.; Wen, Y.; Song, S.; Liu, Y.; Yan, H.; Fan, C. A DNA nanostructure-based biomolecular probe carrier platform for electrochemical biosensing. *Adv. Mater.* **2010**, *22*, 4754−4758.
(33) Liu, G.; Wan, Y.; Gau, V.; Zhang, J.; Wang, L.; Song, S.; Fan, C. An Enzyme-Based E-DNA Sensor for Sequence-Specific Detection of Femtomolar DNA Targets. *J. Am. Chem. Soc.* **2008**, *130*, 6820−6825.
(34) Shen, W.; Deng, H.; Gao, Z. Gold nanoparticle-enabled real-time ligation chain reaction for ultrasensitive detection of DNA. *J. Am. Chem. Soc.* **2012**, *134*, 14678−14681.
(35) Zhang, Y.; Guo, Y.; Quirke, P.; Zhou, D. Ultrasensitive single-nucleotide polymorphism detection using target-recycled ligation, strand displacement and enzymatic amplification. *Nanoscale* **2013**, *5*, 5027−5035.
(36) Pedregosa, F.; Varoquaux, G.; Gramfort, A.; Michel, V.; Thirion, B.; Grisel, O.; Blondel, M.; Prettenhofer, P.; Weiss, R.; Dubourg, V.; Vanderplas, J.; Passos, A.; Cournapeau, D.; Brucher, M.; Perrot, M.; Duchesnay, E. Scikit-learn: Machine Learning in Python. *J. Mach. Learn. Res.* **2011**, *12*, 2825−2830.
(37) İstanbul Laboratuvarı ve Görüntüleme. FMF (Ailesel Akdeniz Ateşi). https://www.labistanbul.com.tr/fmf-ailesel-akdeniz-atesi.html (accessed November 20, 2020).
(38) Aksu, K.; Dokuyucu, O.; Ertenli, A. I.; Gul, A.; Karaaslan, Y.; Kasapcopur, O.; Kiraz, S.; Onat, A. M.; Ozdogan, A. H.; Ozbalas, T.; Ozen, S.; Saylan, M.; Senturk, A.; Tatar, M.; Tuna, E.; Turanlı, M.; Yalcınkaya, F. Cost of Familial Mediterranean Fever (FMF) Disease In Turkey. *Value Health* **2015**, *18*, A666.
(39) Prevention Genetics. Familial Mediterranean Fever (Renal Amyloidosis) via the MEFV Gene. https://www.preventiongenetics.com/testInfo?val=Familial+Mediterranean+Fever+Renal+Amyloidosis+via+the+MEFV+Gene (accessed November 20, 2020).

https://dx.doi.org/10.1021/acssensors.0c02130
ACS Sens. 2021, 6, 950−957